Inherent Promotion of Ionic Conductivity via Coherent Vibrational Strong Coupling of Water

Tomohiro Fukushima, Soushi Yoshimitsu, Kei Murakoshi*

Department of Chemistry, Faculty of Science, Hokkaido University, Sapporo,

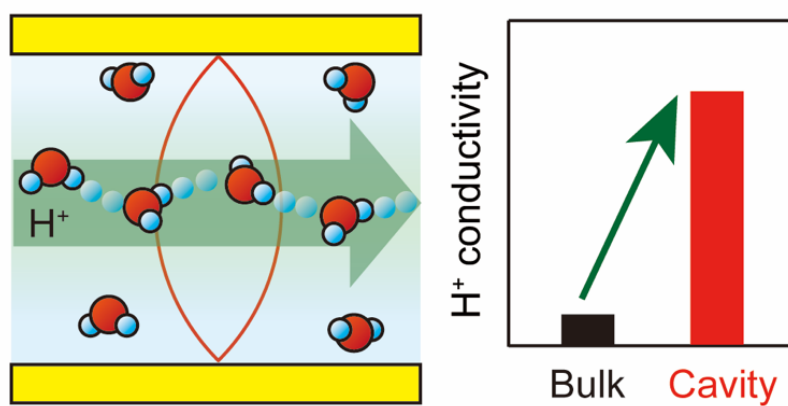Hokkaido, 060-0810, Japan.

Corresponding Author

*kei@sci.hokudai.ac.jp

ABSTRACT

Hydrogen bonding interactions among water molecules play a critical role in chemical reactivity, dynamic proton mobility, static dielectric behavior, and thermodynamic properties of water. In this study, we demonstrate the modification of ionic conductivity of water via hybridization with vacuum electromagnetic field by strongly coupling O–H stretching mode of H_2O to a Fabry–Perot cavity mode. This leads to formation of collective vibro-polaritonic states which, as experiments show, enhances the proton conductivity does increase by an order of magnitude at resonance. In addition, an increase of dielectric constants is observed at resonance in the coupled state. Our finding illustrates

that the potential of engineering a vacuum electromagnetic environment to control the

ground-state properties of water.

TOC GRAPHICS

Introduction

The strong coupling between molecular transition and optical resonator vacuum electromagnetic fields can be used to transform molecular or material properties through the formation of collective hybrid light-matter states; for example, reaction coordinates can be modified by facilitating coherent interactions between individual molecules.[1–4] When electronic excitations are coupled to electromagnetic fields, it has been shown that it can produce unusual photochemical dynamics,[5, 6] enhanced electronic transport,[7, 8] and distinct optical responses.[9, 10] Similarly, vibrational excitation can also be coupled to the vacuum field of a cavity, thus generating so-called vibro-polaritonic states (Figure 1a).[11–13] This is typically achieved by coupling a given vibration to the electromagnetic field of cavity consisting of two parallel mirrors, a Fabry-Perot cavity. The electromagnetic field is generated by the zero-point fluctuation, the so-called vacuum fluctuations, of the cavity mode and therefore occurs even in the dark. Vibrational strong coupling enables transformation of energy landscape in chemical reaction.[14, 15]

Water is typically characterized with representative physicochemical properties such as chemical reactivity, hydration, and thermodynamic properties.[16–18] Even under static conditions, protons are moving along a hydrogen bond network via proton transfer and reorientation between water molecules (Figure 1b); this process is known as the Grotthuss

mechanism.[19–29] A central proposition of using vibrational strong coupling can be the modification of the potential energy surface of water molecules.[30–33] Thus, the proton transfer process and orientation of water molecules in the Grotthuss mechanism can be perturbed by vibrational strong coupling. However, there have been no reports of using vibrational strong coupling to influence the fundamental ionic transport properties of aqueous electrolyte solutions.

In this study, we describe how the vibrational strong coupling of water enhances ionic conductivity and modifies dielectric property. We fabricated a Fabry–Perot cavity for the infrared (IR) and electrochemical measurements. The Rabi splitting of vibrational energy levels was measured for the water of aqueous electrolyte solutions from IR spectra measurements. Interestingly, vibrational strong coupling promotes an order of magnitude increase in the proton conductivity, which was also associated with increased dielectric constants of the electrolyte solutions. The origin of these findings is discussed with respect to vibrational strong coupling regime. Tailoring the intramolecular interactions and coherent dynamics of molecular ensembles play a role in the observed modification of the physicochemical properties of water molecules.
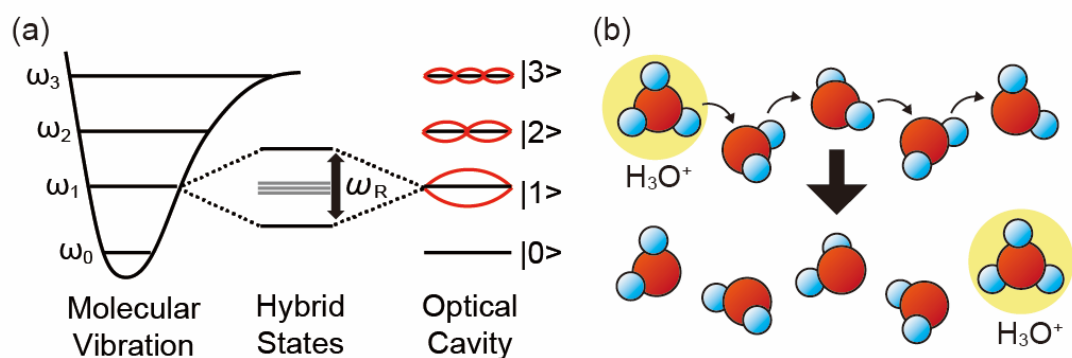
Figure 1. (a) Schematic outline of vibrational strong coupling. The vibrational energy level and cavity energy level were hybridized to form two polaritonic states and dark states. Polaritonic states are separated by the Rabi splitting frequency, ω_R. (b) Mechanistic model for proton transfer among water molecules. Protons in hydronium ions (H_3O^+) are transferred to neighboring water molecules via proton transfer. Sequential reorientation of the hydronium ion yields proton transfer to the next water molecules.

Results and Discussion

A cavity with two parallel mirrors was prepared, as shown in Figure S1. The holes for liquid insertion were used to position the two platinum wire electrodes for electrochemical measurements. The mirrors were fabricated by depositing 20-nm-thick SiO_2 and 8-nm-thick Au on a 2-mm-thick CaF_2 window. These mirrors were mounted within a homemade cell, and the cavity thickness was mechanically controlled by the four

screws. The homogeneity of the cavity thickness was verified based on the Newton ring

as a result of interference structural color of the cavity.[33] The cavity modes can be

determined by the fringe observed in the peak-to-peak separation of cavity modes. The

cavity thickness was controlled between 1 and 5 μm without using a spacer. Typical

spectroscopic properties of the cavity used in this study are shown in Figure S2. The

progression of cavity modes was caused by the interference characteristic of the cavity.

It should be noted that to carry out the electrochemical experiments, the use of polymer

spacers under pressure to tune the cavity is a problem because it deforms the mirrors, and

hence the conductivity is not that of a laterally uniform cavity. The two mirrors had to be

positioned in parallel within the cavity to accurately observe changes in the

electrochemical properties of the electrolyte solutions, as described later.

The formation of vibrational strong coupling states was confirmed using IR

transmission spectroscopy. Water was sandwiched between the two parallel mirrors, and

the IR spectra were recorded as shown in Figure 2a. The first-order cavity mode

frequency was detuned by varying the cavity thickness within the range from 1.0 to 1.6

μm. To characterize the cavity, the coupled cavity mode position was determined based

on one of the uncoupled cavity modes where water had no IR absorption bands of water

molecules. When the cavity mode was matched to the O–H stretching frequency of H_2O

($\omega_{st,OH}$ = 3400 cm^{-1}), the original absorption peak disappeared, and then two new peaks

that were attributed to the vibro-polaritonic states appeared. This observation was

consistent with previous reports about the vibrational strong coupling of H_2O.[30–35] When

the peak position of vibro-polaritonic peaks are plotted as function of the cavity mode,

the expected anti-crossing behavior of the upper and lower polaritonic branches is

observed, as shown in Figure 2b. This Rabi splitting behavior was observed for the first-

order cavity modes without saturation of the intense O–H stretching band. The Rabi

splitting frequency ($\omega_{R,OH}$) was estimated to be 760 cm^{-1}, which is greater than width of

full width at half maximum (FWHM) of the O–H stretching mode (510 cm^{-1}) and the

cavity mode (200 cm^{-1}). In cases with strong coupling conditions, $\omega_{R,OH}$ was greater than

the sum of the photon loss rate of the cavity and the dephasing rate of the O–H stretching

frequency of H_2O molecules.[30–37] This system achieved a particularly vibrational

ultrastrong coupling, where $\omega_{R,OH} / 2\omega_{st,OH} = 0.11$, which can be the benchmark among

molecules coupled to vacuum fields. We also confirmed the vibrational strong coupling

of D_2O as shown in Figure S3. When the cavity mode was matched to the O–D stretching

frequency of D_2O ($\omega_{st,OD}$ = 2500 cm^{-1}), the Rabi splitting frequency was determined to be

520 cm^{-1}. This system also achieved a particularly vibrational strong coupling, where

$\omega_{R,OD} / 2\omega_{st,OD} = 0.11$, which can be the benchmark among molecules coupled to vacuum

fields. We also observed vibro-polaritonic behavior of mixture of H_2O and D_2O (1:1 ratio) as shown in Figure S4. When the cavity mode was matched to either O–H or O–D stretching frequency of mixture of H_2O and D_2O (1:1 ratio), the Rabi splitting for O–H or O–D stretching mode were observed: $\omega_{R,OH} = 500$ cm^{-1} ; $\omega_{R,OD} = 380$ cm^{-1}. In both case, coupling strength was not reaching to the ultrastrong coupling regime ($\omega_{R,OH} / 2\omega_{st,OH} <$ 0.1, $\omega_{R,OD} / 2\omega_{st,OD} < 0.1$). The narrower Rabi splitting frequency can be explained by the lower concentration of H_2O or D_2O species in the cavity. These observations possess the formation of vibrational strong coupling state of water molecules in a cavity.
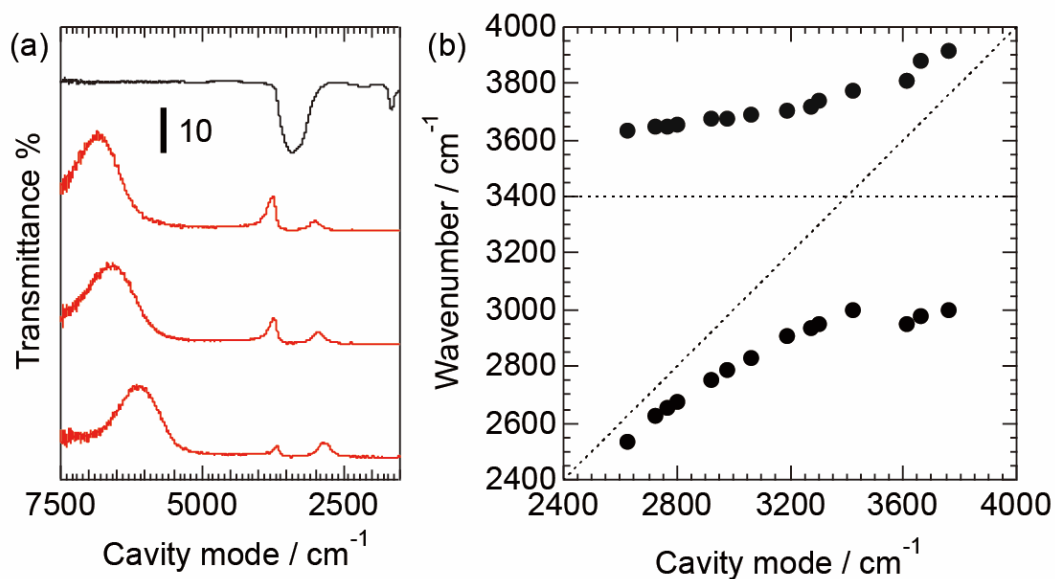
Figure 2. (a) IR spectra of H_2O in a non-cavity cell (black) and H_2O in the cavity cell under detuning conditions (red). From top to bottom, the cavity mode frequency was set as 3420 cm^{-1}, 3300 cm^{-1}, and 3050 cm^{-1}. (b) The anti-crossing behavior of water in the cavity. Cavity thickness was controlled to be between 1.0 and 1.6 μm.

The ionic properties of a 0.01 M $HClO_4$ aqueous electrolyte solution were evaluated under vibrational strong coupling from electrochemical impedance measurements using two platinum electrodes. First, the control experiment was conducted using a non-cavity cell with CaF_2 windows without Au mirrors, where there were no effects of vibrational strong coupling on the ionic conductivity and dielectric constants. Figure S5 shows the typical Cole–Cole plot in the presence and absence of a cavity effect. Both cases involved

9

an equivalent circuit comprising a series of resistance components and two sequential

Randles circuits, which are parallel circuits consisting of resistance and capacitance, as

shown in the inset of Figure S5. A resistance value could then be assigned to the electrical

resistance of the circuit. One Randles circuit was assigned to the electrolyte, and the other

Randles circuit was assigned to the electrode-electrolyte interface. Using the cavity-type

cell, we observed a marked decrease in the resistance and a marginal increase in the

capacitance compared with those observed in the non-cavity-type cell with similar cell

constants. The resistance and capacitance of the 0.01 M $HClO_4$ electrolyte in the cavity

cell solution were 0.720 MΩ and 0.198 pF, respectively. Conversely, the resistance and

capacitance of the 0.01 M $HClO_4$ electrolyte in the non-cavity cell were 3.59 MΩ and

0.182 pF, respectively. Considering that the cell constants of the non-cavity

electrochemical cell and the cavity cell were similar to one another, it could be concluded

that the observed changes in the resistance and capacitance reflect the modification of the

ionic conductivities (σ) and relative dielectric constants (ε) of the electrolyte solution in

the cavity under vibrational strong coupling. It should be noted that the mirrors of the

cavity are coated with SiO_2. In fact, we conducted the control experiments on the CaF_2,

Au / CaF_2, SiO_2 / Au / CaF_2 windows as shown in Figure S6. The observed behavior

suggesting that SiO_2 serves as an insulator for Au mirror.

Next, we measured the proton conductivity of aqueous electrolyte all the while tuning the cavity mode. The proton conductivity of the 0.01 M $HClO_4$ electrolyte with an off-resonance geometry condition was typical value of 0.013 S cm^{-1}.[38, 39] However, as can be found in Figure 3a, when the first and the second cavity modes were tuned across the O–H stretching mode, the proton conductivity was enhanced by an order of magnitude (0.19 S cm^{-1}) under on-resonance vibrational strong coupling conditions with a cavity length of 1.1 μm. The increase of the proton conductivity was again observed at second order of cavity mode at 2.2 μm. In addition, the relative dielectric constants showed a weak dependence: going from 82 for off-resonance condition to 120 for the on-resonance condition under vibrational strong coupling (Figure 3b). The increase of the both ionic conductivity and dielectric constant were confirmed from cavity mode response as shown in Figure S7. Moreover, the unique coupling effect between the O–H vibration and the cavity was confirmed from the control experiment with deuterated 0.01 M $DClO_4$ / D_2O solution. The resonance conditions to achieve the vibrational strong coupling is shifted to the 1.5 μm of cavity length as shown in Figure 3c and Figure 3d, because of the different vibrational frequency ($\omega_{st,OH} = 3400$ cm^{-1}, $\omega_{st,OD} = 2500$ cm^{-1}). The maximum enhancement of the deuteron conductivity reached 0.14 S cm^{-1} with a cavity length of 1.5 μm, as shown in Figure 3c. The modulation of the dielectric response of deuteron was also shifted due

11

to the isotope effects, as shown in Figure 3b and Figure 3d. In addition, we conducted the electrochemical experiments for the $HClO_4$ / $DClO_4$ in H_2O / D_2O (1 : 1 ratio). As described above, the 1 : 1 mixture of H_2O and D_2O showed weaker coupling region to either pure H_2O or D_2O solvent. In these systems, enhancement of the ionic conductivity of $HClO_4$ / $DClO_4$ in H_2O / D_2O (1 : 1 ratio) in cavity under on-resonance condition was low as shown in Figure S8. The observed cavity-dependent behavior of the ionic conductivity excludes the possibility of surface-enhanced ionic transport via formation of a diffusion layer in the microchannel[40–42] or structured water formation at the walls of the microchannels.[43–45] The observed electrochemical behavior is thus inherently different from previously reported electrochemical phenomena in microchannels.

We also evaluated the effect of the solvent and ions on the vibrational strong coupling behavior to study ionic conductivity and dielectric constants (Figure 3e and 3f). When a tetrabutylammonium perchlorate (TBAClO₄) acetonitrile solution was used, vibrational strong coupling of acetonitrile molecules was not observed in the IR spectra (Figure S9). This result could be due to the relatively weak oscillator strength of the acetonitrile molecule ($f_{osc,CN} = 3.93 \times 10^{-6}$) compared with that of the H_2O molecule ($f_{osc,OH} = 181 \times 10^{-6}$).[34, 46] Considering the comparable molar densities of acetonitrile and water, the anisotropic polarizability of acetonitrile molecules may lead to a limited number of

coupled molecules in the cavity. Thus, it was not possible to observe any effect of the coupling on the ionic conductivity of the TBAClO$_4$ acetonitrile solution (Figure S10). However, the ionic conductivity of an aqueous KCl solution showed an increase from 0.001 to 0.004 S cm^{-1} under vibrational strong coupling, as shown in Figure S11a. We did observe a marked enhancement of the ionic conductivity of Milli-Q water over an order of magnitude under vibrational strong coupling, as shown in Figure S11b. The observed modest enhancement with KCl was attributed to the vehicle mechanism, where hydrated K$^+$ and Cl$^-$ migrated throughout the solution as ionic carriers. The mobilities of hydrated K$^+$ and Cl$^-$ also increased under the vibrational strong coupling of water. From these results, we propose that vibrational strong coupling could impact the ground-state proton transfer mechanism.
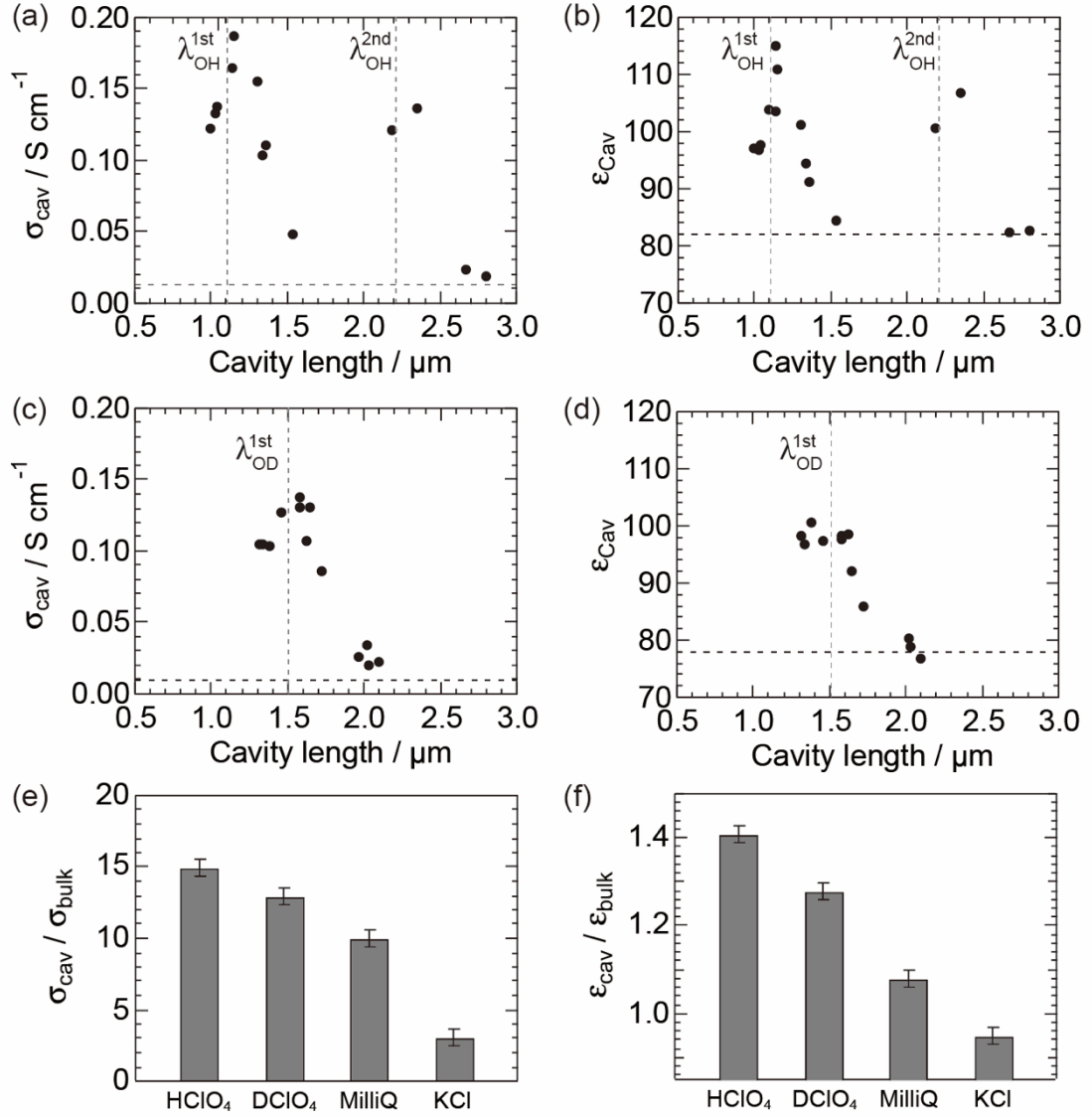
Figure 3. Effect of vibrational strong coupling on (a) ionic conductance and (b) relative

dielectric constants of 0.01 M $HClO_4$ / H_2O electrolyte. (c) Ionic conductance and (d)

relative dielectric constants of 0.01 M $DClO_4$ / D_2O electrolyte. Dotted horizonal lines

represent the bulk values of ionic conductivity and dielectric constant. Dotted vertical

lines represent the resonant wavelength of O－H or O－D stretching mode for the first

or second order of cavity modes. (e) Ionic conductivity and (f) relative dielectric constant for various electrolyte solutions.

We would like to discuss the origin of the modification of ionic conductivities and dielectric constants of aqueous electrolyte solutions under vibrational strong coupling states. Figures 4a and 4b show the dependence of the proton conductivity and dielectric constant on the anti-crossing frequency. This frequency was extrapolated by polaritonic frequency separations at distinct cavity modes.[10, 37] The modulation of both parameters was not observed in the weak coupling region. However, a sudden increase was observed when anti-crossing frequency reaches about 400 cm^{-1} (Figure 4a and 4b). This threshold-like behavior meets the observed strong coupling condition. This observation is consistent with the reported ground-state reactivity modulation under vibrational strong coupling.[47] This dependence plus all the other results presented above show that the origin of the enhancement is vibrational strong coupling.
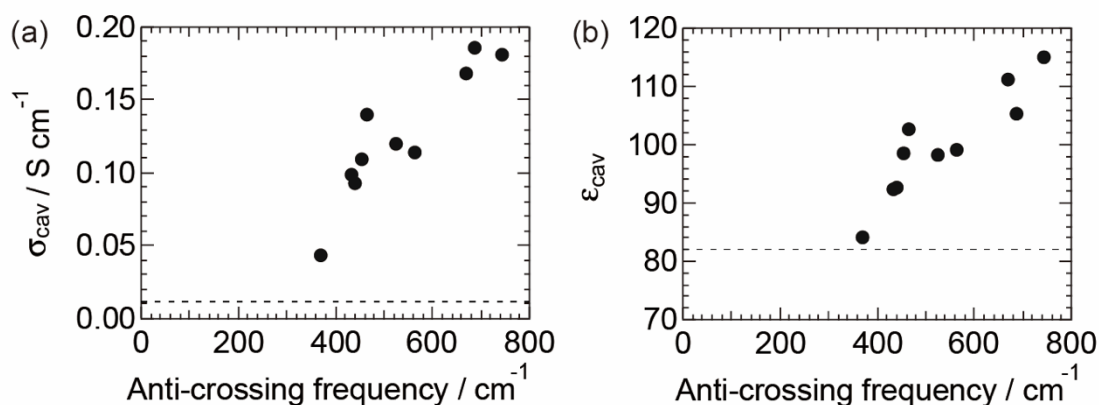
Figure 4. (a) Dependence of proton conductivity of 0.01 M HClO$_4$ on anti-crossing frequency. Red dotted lines are theoretical fitted lines for proton transport in the cavity. Dotted lines are values of bulk proton conductivity. (b) Dependence of dielectric constant of 0.01 M HClO$_4$ on Rabi splitting frequency. Dotted lines are values of bulk dielectric constant.

There is the discussion about the origin of the modification of ground-state properties of molecules under vibrational strong coupling.[4, 48–50] It has been proposed that modification of the potential energy surface to affect the application of transition state theory in vibrational strong coupling.[48, 49] Vibrational strong coupling can modify the ground-state potential energy surface of molecules,[51–55] which can account for the modification of activation energy in the reaction.[4, 56] In addition, the collective strong coupling has been shown to result in coherent emission among molecules micro-meters

16

apart[57, 58] and the coherent vibrational energy transfer process.[59–61] The vibrational strong coupling also affected the coherence among the molecular vibrations of individual water molecules. The formation of the dark states, involved in the Tavis-Cummings model for the energy states in the strong coupling system, could be considered to play some role in the coherent energy transport of the coupled molecules in the cavity.[62–64]

The mechanism for the proton conductivity is explained by the proton transfer and reorientation of water molecules. The proton transfer in intermediate Zundel type complex are regarded as barrierless due to the quantum nature of the excess proton. The rate-limiting step of this mechanism is the hydrogen bond rearrangement known as "water reorientation".[20, 22–25, 29] Considering the origin of the enhancement in proton conductivity, vibrational strong coupling affected the O–H stretching mode by causing softening (lower polariton) and hardening (upper polariton) vibro-polaritonic modes of water.[30–32] Based on the modification of the potential energy surface, collective vibrational strong coupling leads to the accelerated processes of nuclear motion or water reorientation process on the hydration shell under the protons/ions trasnportation.[55, 65–69] Probably, nuclear coherence among water molecules is required for effective charge diffusion and thus ion transport.[70, 71] In addition, the origin of the enhancement in dielectric constant is related to the correlation of the dipoles of individual water molecules.[72–75] We may expect that the

contribution of the dark states could act as an energy reservoir to extend the coherence to modification of the proton transfer rate as well as increase the dielectric constants.[62, 63, 76, 77] The modification of the responses of molecular systems under the perturbations requires novel theoretical consideration for further quantitative descriptions about the present observation.

In principle, the results of this study can be applied to various ionic conductors. Aqueous electrolyte solutions are often used in electrolyzes or fuel cells. Enhancing the proton conductivity or modulating the transport number in such systems is critical. To date, ionic conductors have generally been designed according to the ion binding energy and ionic carrier,[78] and even nanostructures can be exploited by introducing a space-charge layer.[79] Vibrational structures are ubiquitously observed in all types of molecular, polymeric, and inorganic materials. Various types of materials can be placed in an optical cavity, such as that developed in this study. Increasing the ionic conductivity is advantageous for all electrochemical energy devices, such as those applied in water electrolysis, fuel cells, and battery systems. Also, modulating the coherence of proton mobility could also promote various electrochemical reactions coupled to proton transfers. Taking advantage of vibrational strong coupling can aid in the development of efficient energy conversion systems using vibrational strong coupling.

Conclusions

The results presented in this study confirm that the collective vibrational strong coupling of water enhances proton conductivity by an order of magnitude. We also observed the increments in the ionic conductivity of various aqueous electrolyte solutions under vibrational strong coupling of water. The origin of the phenomenon was discussed considering the water molecule behavior in the collective vibro-polaritonic states. Because vibrational structures are ubiquitous in all types of materials, we propose that inherent promotion of ionic transport can be attained using a collective vibrational strong coupling-based approach.

ACKNOWLEDGMENT

REFERENCES

1.   Ebbesen TW. Hybrid Light-Matter States in a Molecular and Material Science Perspective. *Acc Chem Res* **49**, 2403-2412 (2016).

2.   Hertzog M, Wang M, Mony J, Borjesson K. Strong light-matter interactions: a new direction within chemistry. *Chem Soc Rev* **48**, 937-961 (2019).

3.   Garcia-Vidal FJ, Ciuti C, Ebbesen TW. Manipulating matter by strong coupling to vacuum fields. *Science* **373**, 1-9 (2021).

4.   Nagarajan K, Thomas A, Ebbesen TW. Chemistry under Vibrational Strong Coupling. *J Am Chem Soc* **143**, 16877-16889 (2021).

5.   Hutchison JA, Schwartz T, Genet C, Devaux E, Ebbesen TW. Modifying chemical landscapes by coupling to vacuum fields. *Angew Chem Int Ed Engl* **51**, 1592-1596 (2012).

6.   Schwartz T, Hutchison JA, Leonard J, Genet C, Haacke S, Ebbesen TW. Polariton dynamics under strong light-molecule coupling. *ChemPhysChem* **14**, 125-131 (2013).

7.   Orgiu E, *et al*. Conductivity in organic semiconductors hybridized with the vacuum field. *Nat Mater* **14**, 1123-1129 (2015).

8.   Nagarajan K, *et al*. Conductivity and Photoconductivity of a p-Type Organic Semiconductor under Ultrastrong Coupling. *ACS Nano* **14**, 10219-10225 (2020).

9.   Nagasawa F, Takase M, Murakoshi K. Raman Enhancement via Polariton States Produced by Strong Coupling between a Localized Surface Plasmon and Dye Excitons at Metal Nanogaps. *J Phys Chem Lett* **5**, 14-19 (2014).

10.   Kato F, Minamimoto H, Nagasawa F, Yamamoto YS, Itoh T, Murakoshi K. Active Tuning of Strong Coupling States between Dye Excitons and Localized Surface Plasmons via Electrochemical Potential Control. *ACS Photonics* **5**, 788-796 (2018).

11.   Long JP, Simpkins BS. Coherent Coupling between a Molecular Vibration and Fabry–Perot Optical Cavity to Give Hybridized States in the Strong Coupling Limit. *ACS Photonics* **2**, 130-136 (2014).

12.   Shalabney A, George J, Hutchison J, Pupillo G, Genet C, Ebbesen TW. Coherent coupling of molecular resonators with a microcavity mode. *Nat Commun* **6**, 5981 (2015).

13. George J, Shalabney A, Hutchison JA, Genet C, Ebbesen TW. Liquid-Phase Vibrational Strong Coupling. *J Phys Chem Lett* **6**, 1027-1031 (2015).

14. Thomas A, *et al*. Ground-State Chemical Reactivity under Vibrational Coupling to the Vacuum Electromagnetic Field. *Angew Chem Int Ed Engl* **55**, 11462-11466 (2016).

15. Thomas A, *et al*. Tilting a ground-state reactivity landscape by vibrational strong coupling. *Science* **363**, 615-619 (2019).

16. Eisenberg D, Kauzmann W. Structure and Properties of Water. (1969).

17. Ohmine I, Tanaka H. Fluctuation, relaxations, and hydration in liquid water. Hydrogen-bond rearrangement dynamics. *Chemical Reviews* **93**, 2545-2566 (2002).

18. Perakis F, *et al*. Vibrational Spectroscopy and Dynamics of Water. *Chem Rev* **116**, 7590-7607 (2016).

19. Grotthuss CJT. Sur la décomposition de l'eau et des corps q'uelle tient en dissolution à l'aide de l'électricité galvanique. *Ann Chim, LVIII*, 54-74 (1806).

20. Conway BE, Bockris JO, Linton H. Proton Conductance and the Existence of the H_3O^+ Ion. *Journal of Chemical Physics* **24**, 834-850 (1956).

21. Wolynes PG. Dynamics of Electrolyte Solutions. *Annual Review of Physical Chemistry* **31**, 345-376 (1980).

22. Tuckerman M, Laasonen K, Sprik M, Parrinello M. Ab initio molecular dynamics simulation of the solvation and transport of hydronium and hydroxyl ions in water. *The Journal of Chemical Physics* **103**, 150-161 (1995).

23. Agmon N. The Grotthuss mechanism. *Chemical Physics Letters* **244**, 456-462 (1995).

24. Eigen M, Maeyer LD. Self-dissociation and protonic charge transport in water and. *Proceedings of the Royal Society of London Series A Mathematical and Physical Sciences* **247**, 505-533 (1997).

25. Marx D, Tuckerman ME, Hutter J, Parrinello M. The nature of the hydrated excess proton in water. *Nature* **397**, 601-604 (1999).

26. Krishtalik LI. The mechanism of the proton transfer: an outline. *Biochim Biophys Acta* **1458**, 6-27 (2000).

27. Kreuer KD. On the complexity of proton conduction phenomena. *Solid State Ionics* **136**, 149-160 (2000).

28. Cukierman S. Et tu, Grotthuss! and other unfinished stories. *Biochim Biophys Acta* **1757**, 876-885 (2006).

29. Tuckerman ME, Marx D, Parrinello M. The nature and transport mechanism of hydrated hydroxide ions in aqueous solution. *Nature* **417**, 925-929 (2002).

30. Vergauwe RMA, *et al*. Modification of Enzyme Activity by Vibrational Strong Coupling of Water. *Angew Chem Int Ed Engl* **58**, 15324-15328 (2019).

31. Lather J, George J. Improving Enzyme Catalytic Efficiency by Co-operative Vibrational Strong Coupling of Water. *J Phys Chem Lett* **12**, 379-384 (2021).

32. Hirai K, Ishikawa H, Chervy T, Hutchison JA, Uji IH. Selective crystallization via vibrational strong coupling. *Chem Sci* **12**, 11986-11994 (2021).

33.   Fukushima T, Yoshimitsu S, Murakoshi K. Vibrational Coupling of Water from Weak to Ultrastrong Coupling Regime via Cavity Mode Tuning. *The Journal of Physical Chemistry C* **125**, 25832-25840 (2021).

34.   Hidefumi H, Atef S, Jino G. *Vibrational Ultra Strong Coupling of Water and Ice* ChemRxiv (2019).

35.   Lather J, Bhatt P, Thomas A, Ebbesen TW, George J. Cavity Catalysis by Cooperative Vibrational Strong Coupling of Reactant and Solvent Molecules. *Angew Chem Int Ed Engl* **58**, 10635-10638 (2019).

36.   Khitrova G, Gibbs HM, Kira M, Koch SW, Scherer A. Vacuum Rabi splitting in semiconductors. *Nature Physics* **2**, 81-90 (2006).

37.   Torma P, Barnes WL. Strong coupling between surface plasmon polaritons and emitters: a review. *Rep Prog Phys* **78**, 013901 (2015).

38.   Stokes RH, Robinson RA. Ionic hydration and activity in electrolyte solutions. *J Am Chem Soc* **70**, 1870-1878 (1948).

39.   Bockris JOM, Reddy AKN. Modern Electrochemistry 1: Ionics.

40.   Stein D, Kruithof M, Dekker C. Surface-charge-governed ion transport in nanofluidic channels. *Phys Rev Lett* **93**, 035901 (2004).

41.   Plecis A, Schoch RB, Renaud P. Ionic transport phenomena in nanofluidics: experimental and theoretical study of the exclusion-enrichment effect on a chip. *Nano Lett* **5**, 1147-1155 (2005).

42.   Bocquet L, Charlaix E. Nanofluidics, from bulk to interfaces. *Chem Soc Rev* **39**, 1073-1095 (2010).

43.   Tsukahara T, Hibara A, Ikeda Y, Kitamori T. NMR study of water molecules confined in extended nanospaces. *Angew Chem Int Ed Engl* **46**, 1180-1183 (2007).

44.   Chinen H, *et al*. Enhancement of proton mobility in extended-nanospace channels. *Angew Chem Int Ed Engl* **51**, 3573-3577 (2012).

45.   Mawatari K, Isogai K, Morikawa K, Ushiyama H, Kitamori T. Isotope Effect in the Liquid Properties of Water Confined in 100 nm Nanofluidic Channels. *J Phys Chem B* **125**, 3178-3183 (2021).

46.   Ikawa S-I, Maeda S. Infrared intensities of the stretching and librational bands of H_2O, D_2O, and HDO in solids. *Spectrochimica Acta Part A: Molecular Spectroscopy* **24**, 655-665 (1968).

47.   Thomas A, *et al*. Ground state chemistry under vibrational strong coupling: dependence of thermodynamic parameters on the Rabi splitting energy. *Nanophotonics* **9**, 249-255 (2020).

48.   Simpkins BS, Dunkelberger AD, Owrutsky JC. Mode-Specific Chemistry through Vibrational Strong Coupling (or A Wish Come True). *The Journal of Physical Chemistry C* **125**, 19081-19087 (2021).

49.   Wang DS, Yelin SF. A Roadmap Toward the Theory of Vibrational Polariton Chemistry. *ACS Photonics* **8**, 2818-2826 (2021).

50.   Yuen-Zhou J, Xiong W, Shegai T. Polariton chemistry: Molecules in cavities and plasmonic media. *J Chem Phys* **156**, 030401 (2022).

51. Flick J, Appel H, Ruggenthaler M, Rubio A. Cavity Born-Oppenheimer Approximation for Correlated Electron-Nuclear-Photon Systems. *J Chem Theory Comput* **13**, 1616-1625 (2017).

52. Li TE, Nitzan A, Subotnik JE. On the origin of ground-state vacuum-field catalysis: Equilibrium consideration. *J Chem Phys* **152**, 234107 (2020).

53. Galego J, Climent C, Garcia-Vidal FJ, Feist J. Cavity Casimir-Polder Forces and Their Effects in Ground-State Chemical Reactivity. *Physical Review X* **9**, (2019).

54. Li X, Mandal A, Huo P. Cavity frequency-dependent theory for vibrational polariton chemistry. *Nat Commun* **12**, 1315 (2021).

55. Li X, Mandal A, Huo P. Theory of Mode-Selective Chemistry through Polaritonic Vibrational Strong Coupling. *J Phys Chem Lett* **12**, 6974-6982 (2021).

56. Hirai K, Hutchison JA, Uji IH. Recent Progress in Vibropolaritonic Chemistry. *ChemPlusChem* **85**, 1981-1988 (2020).

57. Guebrou SA, *et al*. Coherent emission from a disordered organic semiconductor induced by strong coupling with surface plasmons. *Phys Rev Lett* **108**, 066401 (2012).

58. Shi L, Hakala TK, Rekola HT, Martikainen JP, Moerland RJ, Torma P. Spatial coherence properties of organic molecules coupled to plasmonic surface lattice resonances in the weak and strong coupling regimes. *Phys Rev Lett* **112**, 153002 (2014).

59.   Dunkelberger AD, Spann BT, Fears KP, Simpkins BS, Owrutsky JC. Modified relaxation dynamics and coherent energy exchange in coupled vibration-cavity polaritons. *Nat Commun* **7**, 13504 (2016).

60.   Xiang B, *et al*. Intermolecular vibrational energy transfer enabled by microcavity strong light-matter coupling. *Science* **368**, 665-667 (2020).

61.   Grafton AB, *et al*. Excited-state vibration-polariton transitions and dynamics in nitroprusside. *Nat Commun* **12**, 214 (2021).

62.   Vurgaftman I, Simpkins BS, Dunkelberger AD, Owrutsky JC. Negligible Effect of Vibrational Polaritons on Chemical Reaction Rates via the Density of States Pathway. *J Phys Chem Lett* **11**, 3557-3562 (2020).

63.   Scholes GD, DelPo CA, Kudisch B. Entropy Reorders Polariton States. *J Phys Chem Lett* **11**, 6389-6395 (2020).

64.   Botzung T, Hagenmuller D, Schutz S, Dubail J, Pupillo G, Schachenmayer J. Dark state semilocalization of quantum emitters in a cavity. *Physical Review B* **102**,   (2020).

65.   Yang PY, Cao J. Quantum Effects in Chemical Reactions under Polaritonic Vibrational Strong Coupling. *J Phys Chem Lett* **12**, 9531-9538 (2021).

66.   Campos-Gonzalez-Angulo JA, Yuen-Zhou J. Polaritonic normal modes in transition state theory. *J Chem Phys* **152**, 161101 (2020).

67.   Bernal JD, Fowler RH. A theory of water and ionic solution, with particular reference to hydrogen and hydroxyl ions. *Journal of Chemical Physics* **1**, 515-548 (1933).

68.   Stearn AE, Eyring H. The deduction of reaction mechanisms from the theory of absolute rates. *Journal of Chemical Physics* **5**, 113-124 (1937).

69.   Steam AE, Irish EM, Eyring H. A Theory of Diffusion in Liquids. *The Journal of Physical Chemistry* **44**, 981-995 (2002).

70.   Murch GE. The Haven Ratio in Fast Ionic Conductors. *Solid State Ionics* **7**, 177-198 (1982).

71.   Dippel T, Kreuer KD. Proton Transport Mechanism in Concentrated Aqueous-Solutions and Solid Hydrates of Acids. *Solid State Ionics* **46**, 3-9 (1991).

72.   Hubbard J, Onsager L. Dielectric dispersion and dielectric friction in electrolyte solutions. I. *The Journal of Chemical Physics* **67**, 4850-4857 (1977).

73.   Chandra A. Static dielectric constant of aqueous electrolyte solutions: Is there any dynamic contribution? *The Journal of Chemical Physics* **113**, 903-905 (2000).

74.   Onsager L. Electric Moments of Molecules in Liquids. *Journal of the American Chemical Society* **58**, 1486-1493 (2002).

75.   Zhang C, Hutter J, Sprik M. Computing the Kirkwood g-Factor by Combining Constant Maxwell Electric Field and Electric Displacement Simulations: Application to the Dielectric Constant of Liquid Water. *J Phys Chem Lett* **7**, 2696-2701 (2016).

76.   Campos-Gonzalez-Angulo JA, Ribeiro RF, Yuen-Zhou J. Resonant catalysis of thermally activated chemical reactions with vibrational polaritons. *Nat Commun* **10**, 4685 (2019).

77. Du M, Campos-Gonzalez-Angulo JA, Yuen-Zhou J. Nonequilibrium effects of cavity leakage and vibrational dissipation in thermally activated polariton chemistry. *J Chem Phys* **154**, 084108 (2021).

78. Kreuer K-D. Proton Conductivity: Materials and Applications. *Chemistry of Materials* **8**, 610-641 (1996).

79. Maier J. Nanoionics: ion transport and electrochemical storage in confined systems. *Nat Mater* **4**, 805-815 (2005).